2.2. BIO-OPTICAL MODEL DESCRIPTION

In this section, a bio-optical model is developed for case II waters in the Lucinda region, Great Barrier Reef, Australia. The model is based on analytical and empirical relationships between concentrations of optically significant substances and remote sensing water reflectance, which are derived from the current ocean colour modelling literature. A method of inverting the remote sensing signal to concentrations of water-colouring substances is then introduced.

2.2.1. SeaWiFS water-leaving radiance

The total upward reflectance at the top of the ocean–atmosphere system $\rho_t(\lambda)$, as measured by the remote sensor at a wavelength λ, is defined by Gordon and Wang (1994) and can be written as

$$\rho_t(\lambda) = \rho_r(\lambda) + \rho_a(\lambda) + \rho_{ra}(\lambda) + \rho_g(\lambda) + T_v(\lambda)\rho_{wc}(\lambda) + T_v(\lambda)\rho_w(\lambda), \quad (2.3)$$

where $\rho_r(\lambda)$ is the reflectance resulting from multiple scattering by air molecules (Rayleigh scattering) in the absence of aerosols; $\rho_a(\lambda)$ is the reflectance resulting from multiple scattering by aerosols in the absence of air; $\rho_{ra}(\lambda)$ is the multiple interaction term between molecules and aerosols; $\rho_g(\lambda)$ is the sun glint reflectance; $\rho_{wc}(\lambda)$ is the reflectance at the sea surface that arise from sunlight and skylight reflecting from whitecaps on the surface; $T_v(\lambda)$ is the viewing diffuse transmittance from sea to sensor; and $\rho_w(\lambda)$ is the water-leaving reflectance – a desired quantity in ocean colour remote sensing.

The normalised water-leaving radiance $nLw(\lambda)$ is the primary ocean product of SeaWiFS and is defined as water-leaving radiance corrected to correspond to a solar zenith angle of zero (i.e. the sun overhead) (McClain et al 1992). It has units of mW/cm^2/μm/sr and is expressed through water-leaving reflectance $\rho_w(\lambda)$, extraterrestrial solar irradiance $F(\lambda)$ and atmospheric diffuse transmittance in the solar direction $t(\lambda,\theta)$ with the solar zenith angle θ (Siegel et al 2000):

$$nLw(\lambda) = \frac{\rho_w(\lambda)F(\lambda)}{\pi t(\lambda,\theta)}. \quad (2.4)$$

To arrive at water-leaving reflectance and subsequently radiance, the first five terms of equation 2.3 must be properly accounted for and subtracted from the total radiance received

by a satellite-borne radiance meter – the task of the so-called atmospheric correction algorithm (Gordon et al 1994). It should be noted, however, that depending on the wavelength, more than 80 % of the signal measured by the remote sensor originates from scattering of the solar beam by air molecules and aerosol particles (dust, water droplets, salt, etc) within the atmosphere (the first three terms in equation 2.3). Therefore, retrieval of water surface quantities is extremely sensitive to correct removal of the atmospheric signal. This issue is addressed further in section 3.2.

2.2.2. Apparent and inherent optical properties

This and the following sections describe analytical and empirical relationships between concentrations of optically significant substances and apparent and inherent optical water properties, which are then combined to develop a semi-analytical bio-optical model, using SeaWiFS visible spectral bands (a flow-chart of the model is shown in Figure 2.1). As a result, spectral water-leaving radiance distributions are described and thus the "forward" problem of ocean optics is addressed.

Normalised water-leaving radiance $nLw(\lambda)$ at 8 spectral bands between 412 nm and 865 nm as derived from SeaWiFS can be converted from remote sensing reflectance $Rrs(\lambda)$ by multiplying it by the wavelength-appropriate bandpass-weighted mean solar irradiance $F(\lambda)$ (Gordon et al 1994):

$$nLw(\lambda) = Rrs(\lambda)\, F(\lambda). \qquad (2.5)$$

Remote sensing reflectance $Rrs(\lambda)$ is defined as the ratio of the upwelling radiance to downwelling irradiance just above the water surface (for units see Appendix 2). In order to relate $Rrs(\lambda)$ to underwater optical properties, it must be transformed into subsurface remote sensing reflectance $r_{rs}(\lambda)$ through the appropriate water-to-air divergence factor, which includes radiance transmittance from above (below) to below (above) the surface, refractive index of water, water-to-air internal reflection, and the ratio of upwelling subsurface irradiance to upwelling subsurface radiance (Lee et al 1998):

$$Rrs(\lambda) = \frac{0.518 r_{rs}(\lambda)}{1 - 1.562 r_{rs}(\lambda)}, \qquad (2.6)$$

where the denominator accounts for the internal reflection of the water–air interface, which is important for very shallow or very turbid waters.

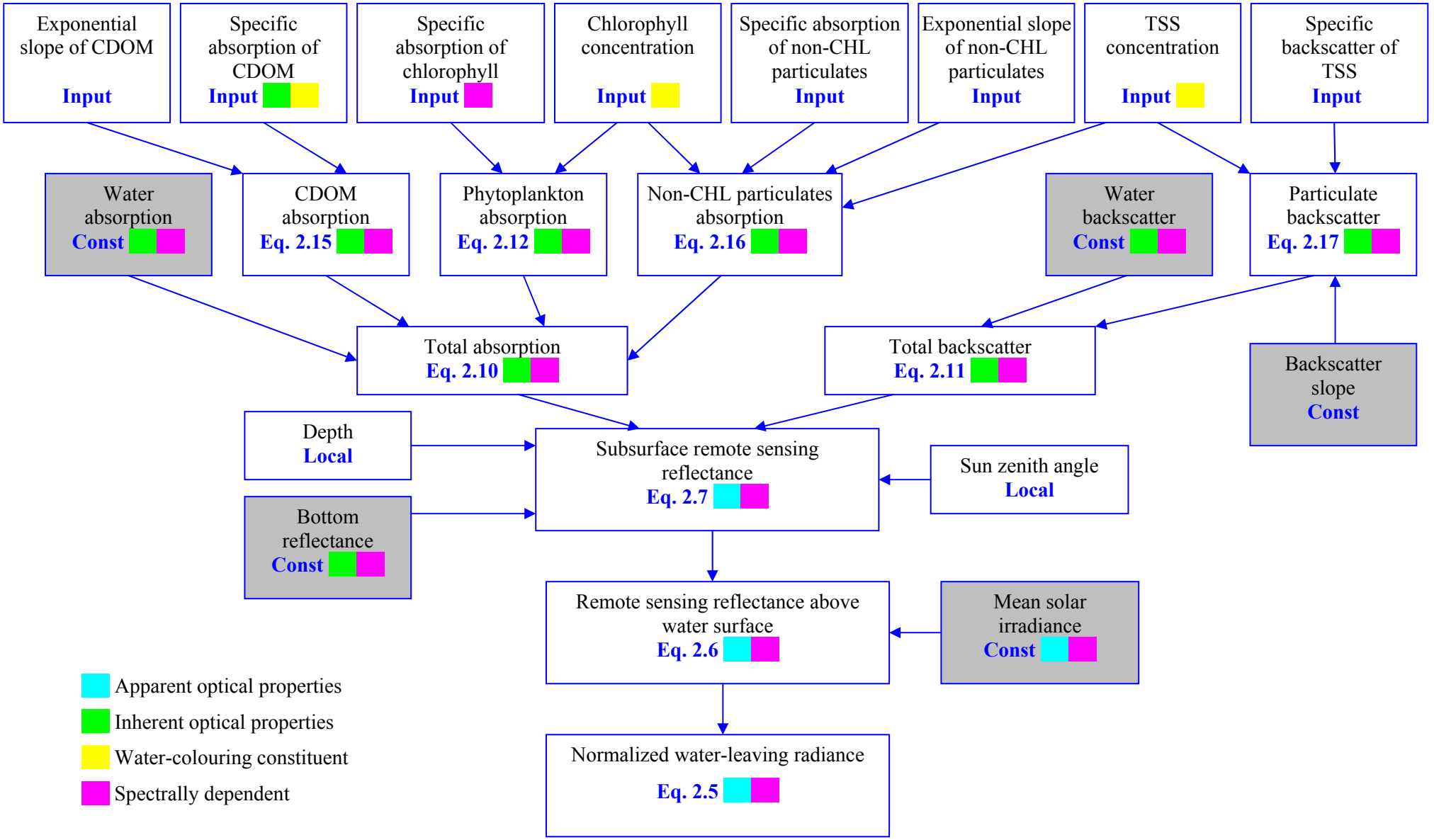

Figure 2.1. Forward bio-optical model diagram. Constant inputs to the model are shaded.

Subsurface remote sensing reflectance $r_{rs}(\lambda)$ is modelled after approximation for optically shallow waters by Lee, Carder et al. (1998) based on their simulations using the Hydrolight radiative transfer numerical model with a particle phase function (i.e. the radiant intensity from a volume element in a given direction per unit of irradiance on the volume and per unit volume) typical of coastal waters:

$$r_{rs}(\lambda) = (0.070 + 0.155u(\lambda)^{0.752})\, u(\lambda)\, (1 - 1.03 \exp\{-[1/\cos(\theta_w) + 1.2\,(1 + 2u(\lambda))^{0.5}]\, \alpha H\}) + 0.31\rho_b(\lambda)\exp\{-[1/\cos(\theta_w) + 1.1\,(1 + 4.9u(\lambda))^{0.5}]\, \alpha H\}; \quad (2.7)$$

$$\alpha = a(\lambda) + bb(\lambda); \quad (2.8)$$

where $u(\lambda)$ is inherent optical properties expression, H is water depth, $\rho_b(\lambda)$ is bottom reflectance, and θ_w is subsurface solar zenith angle (zero for normalised water-leaving radiance).

Here the first bracket on the right-hand side of the equation represents remote sensing reflectance for deep water. $r_{rs}(\lambda)$ is an apparent optical property (AOP) and as such depends on the ambient light conditions (i.e. solar zenith angle). It is also controlled by inherent optical properties (IOP) of the constituents in the water column (reflected in the parameter $u(\lambda)$), bottom reflectance and bottom depth.

Spectral light absorption and backscattering coefficients are the two inherent optical properties directly determining the diffuse reflectance of the ocean. The nature of the relationship between AOP and IOP has been extensively explored by mathematical modelling of the underwater light field (Preisendorfer 1965; Morel et al 1977; Gordon 1986). A simplified version of the radiative transfer theory (Gordon et al 1988) states that reflectance is directly proportional to backscatter, and inversely to the sum of backscatter and absorption in the aquatic media and as such, term $u(\lambda)$ in equation 2.7 is expressed as

$$u(\lambda) = \frac{bb(\lambda)}{a(\lambda) + bb(\lambda)}. \quad (2.9)$$

The additivity principle applies strictly when dealing with inherent optical properties (Jerlov 1976). Consequently, the IOP coefficients can be split into their partial components such as water, phytoplankton, coloured dissolved organic matter, and non-chlorophyllous particulates.

Coefficients $a(\lambda)$ and $bb(\lambda)$ are then expressed as the sum of contributions from these optically significant constituents:

$$a(\lambda) = a_w(\lambda) + a_{ph}(\lambda) + a_{CDOM}(\lambda) + a_{np}(\lambda); \quad (2.10)$$

$$bb(\lambda) = bb_w(\lambda) + bb_{TSS}(\lambda) + bb_{ph}(\lambda). \quad (2.11)$$

Here $a(\lambda)$ represents total absorption, with $a_w(\lambda)$, $a_{ph}(\lambda)$, $a_{CDOM}(\lambda)$ and $a_{np}(\lambda)$ standing for water, chlorophyllous particles, coloured dissolved organic matter, and non-chlorophyllous particulate absorption, respectively. Backscatter is reflected in $bb_w(\lambda)$, $bb_{ph}(\lambda)$ and $bb_{TSS}(\lambda)$, which represent water, chlorophyll and non-chlorophyllous particulate backscattering coefficients, respectively. Values for water absorption were taken from Pope and Fry (1997); and those for water backscatter, which equals one-half of the total scattering coefficient for pure seawater, from Smith and Baker (1981). Other terms are discussed in more detail below.

2.2.3. Absorption of phytoplankton

Phytoplankton (*phyto* is Greek for plant, *planktos* to wander) are unicellular and multicellular microscopic plant organisms that live in the surface waters of the oceans**.** They use sunlight, carbon dioxide and water in a process called photosynthesis (*photo* – light, *synthesis* – build), a process of converting light energy to chemical energy and storing it in the bonds of sugar. Phytoplankton also requires nutrients to produce organic compounds, which are required for building cells.

The principal characteristics that distinguish the major groups of phytoplankton from each other include size, shape, photosynthetic pigments, and cell wall composition. The first three affect the optical signature directly. In terms of size, phytoplankton ranges from below 1 micrometer to over 100 micrometers in diameter. The largest phytoplankton includes such groups as diatoms, coccolithophorids, and dinoflagellates. A single-cell planktonic form of the blue-green algae known as cyanobacteria represents the smallest phytoplankton, so called ultraphytoplankton. The groups are divided into classes and the classes into species.

The feature that gave phytoplankton their name and distinguished these organisms from other substances present in the water is photosynthetic pigments, mainly chlorophyll, which enable living pigmented algal cells to use light energy from the sun and through a chain of transformations to produce their own energy and subsequently synthesise cellular components from carbon dioxide (Kirk 1994). All phytoplankton contain chlorophyll_*a* pigment thus

making it a suitable proxy for determining the quantity of photosynthetic organisms in the water. The pigment is spectrally selective and has distinctive absorption peaks in the green (430 nm, thus the colour is usually green) and orange (663 nm, generally a smaller peak) parts of the visible spectrum. In addition to chlorophyll_*a*, phytoplankton contains a variety of other pigments, e.g. chlorophyll_*b*, chlorophyll _*c*, carotenoids and phycobilins. These are sometimes called accessory pigments because not all of them are present in every phytoplanktonic cell.

Optical properties of phytoplankton are usually described in terms of chlorophyll_*a* absorption as this is the ubiquitous pigment in phytoplankton and also historically it is the proxy for in situ determination of phytoplankton abundance. Throughout the present work the subscript _*a* is dropped from the chlorophyll notation for simplicity, although it should be noted that total chlorophyll concentration (a measure of all types of chlorophyll) does not equal chlorophyll_*a* concentration in most cases.

With all the above in mind and following Bricaud et al (1995, 1998), chlorophyll absorption $a_{ph}(\lambda)$ is calculated as the product of the specific absorption coefficient $a^*_{ph}(\lambda)$ and the concentration of chlorophyll [CHL]:

$$a_{ph}(\lambda) = a^*_{ph}(\lambda)\,[CHL]. \qquad (2.12)$$

Often non-linear flattening of CHL-specific absorption spectra is observed in natural waters as size and cellular pigment concentration increase – a phenomenon typically referred to as the pigment packaging effect (Kirk 1994; Bricaud et al 1995; Bissett et al 1997; Ciotti et al 1999; Lohrenz et al 2003). Therefore, to take into account this packaging effect, spectrum of specific absorption of chlorophyll was allowed to vary in the model so that $a^*_{ph}(443)$ ranged between 0.02 and 0.14 m^2/mg (Table 2.1). This range, as well as specific absorption coefficients at other wavelengths, were obtained from literature sources (Sathyendranath et al 1987; Ahn 1992; Roesler et al 1995; Bricaud et al 1998; Stramski et al 2001; Babin et al 2003; Dupouy et al 2003) and in situ measurements in the Townsville region in October 2002 (Oubelkheir et al 2003). It should be noted that this parameter is independent of chlorophyll concentration.

2.2.4. Backscatter of phytoplankton

The backscatter of phytoplankton $bb_{ph}(\lambda)$ is usually related to CHL concentration through the specific backscatter coefficient of chlorophyll at a reference wavelength $bb^*_{ph}(546)$ and a spectrally dependent term raised to the power υ (Stramski et al 2001), and is parameterised in the following form:

$$bb_{ph}(\lambda) = bb^*_{ph}(546)\,[CHL]\,(546/\lambda)^{\upsilon}. \quad (2.13)$$

The recent study of Vaillancourt et al. (2004) has provided values of backscatter coefficients for 29 species representing 12 classes of cultured marine plankton. Their power slopes υ ranged from 0.005 to 2.32, and the specific backscatter coefficients at 440 nm ranged over an order of magnitude from 0.0002 to 0.003 m^2/mg. The study gave the average power of phytoplankton backscatter as 1.18, similar to that observed for non-chlorophyllous particles (see section 2.2.6 below). This agreement between spectral shapes allows derivation of TSS equivalent of chlorophyll. To determine this relationship, the right sides of equations 2.13 and 2.17 were equated. Considering the estimated average $bb^*_{ph}(550)$ of 0.0009 m^2/mg (Vaillancourt et al 2004), the average specific backscatter of particles as 0.01 m^2/g (section 2.2.6), and assuming the same spectral slopes of backscatter of TSS and CHL, the conversion of CHL to equivalent suspended sediment concentration SS_{CHL} is:

$$[SS_{CHL}] = [CHL]*0.09. \quad (2.14)$$

Since (i) virtually nothing is known about phytoplankton backscatter properties at Lucinda, (ii) spectral shapes of backscatter of phytoplankton and other particulates are similar, and (iii) the model has negligible sensitivity to variations in the backscatter coefficient of phytoplankton (resulting water-leaving radiance variations were below 4 % at all wavelengths, see section 2.3.3), $bb_{ph}(\lambda)$ was included in the total particulate backscatter estimates described in section 2.2.6. It should be noted, however, that possible deviations of the spectral shape of phytoplankton backscatter from that of non-living particles would result in less reliable estimates of chlorophyll concentration. This is particularly relevant at high levels of chlorophyll, e.g. during phytoplankton blooms.

2.2.5. Coloured dissolved organic matter

Coloured, or chromophoric, dissolved organic matter (CDOM), also called “yellow substance”, “gelbstoff”, or “gilvin”, represents the optically active fraction of dissolved organic matter. It is usually comprised of a complex group of polymeric organic compounds

including humic and fulvic acids, and may have a local origin from degradation of phytoplankton cells or other organic particles, as well as be advected from a distant source such as a river. However, precise substances which comprise CDOM in natural waters remain largely undefined (Hansell et al 2002).

As utilised in conventional oceanography, "dissolved" matter is a non-physical term since it is determined by the filter pore size used for in situ determinations of CDOM. Historically, 0.2-1.2 μm filters have been employed to separate dissolved and particulate fractions (Eisma 1993). Material smaller than the filter pore size is considered dissolved, although in reality it may be colloidal or particulate: particles as small as 0.02 μm have been observed in natural waters (Bergh et al 1989). It is therefore important to bear in mind that differentiation between particulate and dissolved matter in oceanography is not physical but rather technical and historically-based.

At present there are no direct methods in ocean science for isolating coloured dissolved organic matter and determining its concentration (Bowers et al 2004). It is therefore customary to characterise the content of CDOM in terms of its optical manifestation. It should be noted, however, that yellow substance and dissolved organic matter (DOM) are not necessarily the same substances, since some DOM can be non-absorbing and thus colourless, and also photooxidative degradation of organic matter by the light ultimately leads to destruction of CDOM but not necessarily DOM (Moran et al 2000; Hansell et al 2002). Therefore, locally derived yellow substance is likely to accumulate more at depth than in surface layers of water bodies. So strictly speaking, CDOM cannot be used as an optical equivalent of DOM or dissolved organic nutrients. However, compositional changes and hence optical variability due to photodegradation can be taken into account by varying the shape and magnitude of the optical signature of CDOM.

As a dissolved matter with small representative size relative to the wavelengths of visible light, CDOM is usually assumed to contribute insignificantly to backscatter. On the other hand, some researchers claim that particles smaller than 0.2 μm strongly affect the backscatter signal (Stramski et al 1991; Stramski et al 2001). Nonetheless, in the present study backscatter of particles smaller than 0.2 μm has been assumed to be negligible.

In contrast, CDOM absorbs strongly in the blue region of the visible spectrum and progressively less towards longer wavelengths, such that in the near-infrared region (0.7-5 μm) its absorbance becomes negligible. Historically, CDOM absorption $a_{CDOM}(\lambda)$ is modelled

after Bricaud, Morel et al. (1981) in an exponential fashion with the reference wavelength 440 nm:

$$a_{CDOM}(\lambda) = a_{CDOM}(440)\ exp\ [S_{CDOM}(\lambda - 440)]. \quad (2.15)$$

CDOM has been found to possess variable absorption properties in different waters around the world. Reference absorption $a_{CDOM}(440)$ can vary from virtually zero in extremely clear open ocean waters to up to several tens of inverse meters encountered in very turbid riverine waters (Green et al 1994). In the latter case CDOM would dominate the absorption by phytoplankton as well as other water optical properties in the blue region of the spectrum. In this scenario, primary productivity would tend to decrease even with the presence of nutrients, because the amount and quality of the photosynthetically active radiation available for phytoplankton is greatly reduced (Hansell et al 2002). Exponential slope S_{CDOM} varies within a relatively narrow range between 0.007 and 0.032 nm^{-1} in natural waters (Bricaud et al 1981; Kopelevich et al 1989; Kirk 1994; Bukata et al 1995; Roesler et al 1995; Nelson et al 1998; Toole et al 2001; Babin et al 2003; Bowers et al 2004; Green et al 2004), with the mean ocean value of 0.015 nm^{-1}. The CDOM exponential slope in the vicinity of Lucinda Point ranged between 0.006 and 0.026 nm^{-1}, with the mean value 0.015 nm^{-1} and standard deviation 0.004 (Figure A8 in Appendix 4). For the Herbert River model, CDOM absorption at 440 nm as well as exponential slope were allowed to vary within ranges expected in the region (Table 2.1).

2.2.6. Inherent optical properties of suspended sediments

Suspended particulate matter in the ocean is probably the most variable optically significant constituent. It may be divided into groups based on origin (e.g. biogenic, terrigenous, atmospheric, volcanic), source (allochtonous, or local, and autochtonous, or brought from outside), composition (inorganic, organic, mixed aggregates), size (e.g. nano-, micro-, macroparticles), physical properties (e.g. density, porosity), etc. For optical applications, composition, size and shape of particles are the most important properties.

Major sources of particles in coastal regions include river advection, wave and/or current resuspension of bottom sediments, local biogenic production, and atmospheric deposition. Sinks involve dispersal by currents and waves, settling by gravity and consumption by organisms. The general trend observed in natural waters is extremely small concentrations in the open ocean (average concentration is circa 0.02 g/m^3) and substantially larger abundances towards the coasts, reaching up to several kg/m^3 in muddy rivers (Eisma 1993).

It is generally recognised that suspended matter in the ocean is present mainly in the form of fragile flocs (Eisma 1993; Ittekkot et al 1996). The term flocculation means the process whereby particles are brought together and remain attached to each other for some time. Large (up to several cm) macro-aggregates of mud and biogenic particles become bound together due to high adsorptivity of clay minerals and organic matter. Therefore they are usually found in more productive areas of the ocean. Suspended matter flocculates at increasing salinity and has been found to occur at salinities between 1 and 7 ‰, depending on the mineralogy of the particles (Eisma 1993). Hence the abundance of flocs is expected to increase in places where river waters mix with seawaters.

The flocculation of suspended particles has a pronounced effect on particle transport and on the optical properties of waters containing flocs. Formation of a large particle out of small ones contributes to increasing its settling rate, which is proportional to the particle diameter squared. However, this can be offset by lower densities of flocs relative to individual particles, when the former contain more organic matter than the fine ones, or when they enclose more water, or both. Therefore, interpreting the abundance and dynamics of these large aggregates in the water is not straightforward, and careful attention must be devoted to their sampling and measurements. Concentration of a large number of fine particles into a few large ones gives greater transparency to the water, which is manifested in reduced the backscattering efficiency of flocs in comparison to individual components.

As with dissolved material, particulates are operationally defined as everything retained on a filter of a certain size (usually 0.7 μm). The dry weight of the particles is called total suspended solid or sediment (TSS) concentration and is usually ascribed g/m^3, or equivalently, mg/L units. It should be noted that TSS includes phytoplankton as well as non-living particulates, and since chlorophyll absorption is expressed by a separate relationship (section 2.2.3), its equivalent concentration in terms of weight should be subtracted from the TSS concentration when estimating non-chlorophyllous particulate absorption. Backscatter of phytoplankton, on the other hand, is included in backscatter of particulates (section 2.2.4), so no adjustments for CHL are necessary.

For particulate absorption, scattering and backscattering estimates, two approaches exist. One is Mie theory, the other is empirical functions. The former is more robust and physically grounded (i.e. universally applicable to natural environments) while the latter is usually more realistic and transparent (i.e. better suited for the region for which a relationship was established). The Mie theory approach presents certain limitations for studying optical

properties of suspended matter in natural waters due to various assumptions inherent in the theory and introduced by the measurement procedures, such as (i) lack of knowledge of the imaginary part of the refractive index, (ii) assumption of the same particle size distribution for organic and inorganic fractions, and (iii) the fact that suspended matter is present in the water mainly in the form of fragile flocs (Stramski et al 2001; Twardowski et al 2001; Risovic 2002; Babin et al 2003; Green et al 2003). Therefore, the empirical functions approach was chosen in the present study to express the inherent optical properties of suspended sediments.

Little has been published on absorption by inorganic sediments, and available information suggests that it is negligible in comparison to organic sediment absorption (Lahet et al 2000). The absorption spectra of non-living organic sediments, or detritus, follow that of CDOM with a slightly shallower exponential slope of the absorption curve (Iturriaga et al 1989; Roesler et al 1989; Carder et al 1991). Therefore, the components are often combined in a single term (Roesler et al 1995; Lee et al 1999). However, in the present work two separate absorption coefficients are used because (i) TSS and CDOM are different final products, and (ii) the exponential slopes have different ranges for particulate and dissolved matter. The absorption of non-chlorophyllous particulates $a_{np}(\lambda)$ decreases exponentially with increasing wavelength according to the shape factor S_{np}:

$$a_{np}(\lambda) = a^*_{np} [TSS - SS_{CHL}] \exp [S_{np}(\lambda - 440)]. \quad (2.16)$$

Here $[TSS\text{-}SS_{CHL}]$ is chlorophyll-corrected TSS concentration (for SS_{CHL} derivations see equation 2.14) and a^*_{np} is specific absorption of non-CHL particulates. In the model, a^*_{np} was varied between 0.001 and 0.04 m^2/g, and S_{np} was varied between 0.005 and 0.013, in accordance with ranges usually encountered in the ocean (Roesler et al 1989; Bricaud et al 1990; Bricaud et al 1998; Toole et al 2001; Babin et al 2003; Bowers et al 2004).

For backscatter of particulates $bb_{TSS}(\lambda)$ a spectral power law model is most commonly assumed (Sathyendranath 2000):

$$bb_{TSS}(\lambda) = bb^*_{TSS} [TSS] (\lambda/546)^{\gamma}. \quad (2.17)$$

In the present model, specific backscatter of suspended sediments bb^*_{TSS} is allowed to vary by one order of magnitude, from 0.002 to 0.02 m^2/g, while the power γ is bounded by 0.8 and 1.25. These ranges are within those found in marine environments (ESA 2002; Babin et al 2003; Oubelkheir et al 2003; Green et al 2004).

2.2.7. Bottom reflection

Light reflected from the sea floor affects ocean colour if optical depth (defined here as the depth at which downward irradiance is attenuated by 90 % relative to subsurface values, also known as the mid-point of the euphotic layer (Kirk 1994)) is below the physical water depth. In other words, the water must be both shallow and clear for bottom signal to be noticeable in water-leaving radiances. This effect varies with substances present in the water column as well as with substrate types.Previous studies have shown that the sea bottom in the vicinity of the Hinchinbrook Channel is characterised by a nearshore sediment wedge of sandy mud which extends offshore to approximately 20 m water depth, seawards of which carbonate sand predominates (Woolfe et al 2000). Another geochemical study of the area revealed that the colour of sandy mud around Lucinda varied from grey-brown to olive-brown (Holmes 1993). Sediment grabs collected in the coastal waters off Lucinda in October 2003 and February 2004 revealed muddy sand to sandy mud variations among samples. Figure 2.2 shows representative sediments in the area from the field data. As (i) all the collected samples were dark-coloured, (ii) estimates of bottom reflectance vary in the literature (Santer et al 1997; Lee et al 1999; Pozdnyakov et al 2003), and (iii) the model is insensitive to bottom reflection at depths below 25 m, the single spectrum of monotonously increasing bottom reflectance from 0.1 at 412 nm to 0.2 at 670 nm was adopted for the whole area studied.

Bottom depths for the region bounded by latitudes 18º 15’ S and 18º 50’ S and longitudes 146º 00’ E 146º 45’ E were manually digitised from the nautical chart of the area (RAN 1990). Operationally, actual bottom depths and adopted bottom reflectance spectra were used as the input to the model (equation 2.7, Figure 2.1).

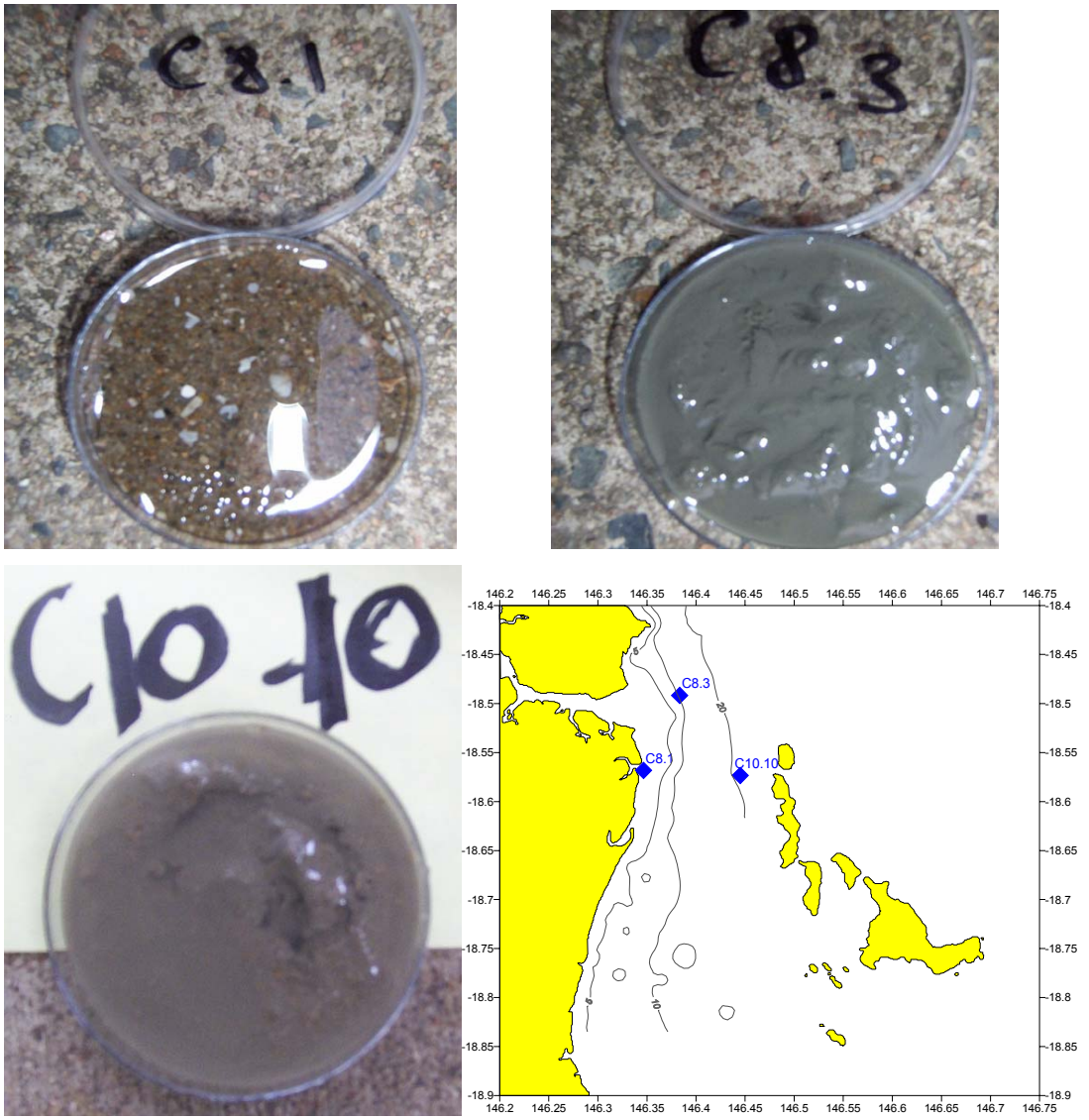

Figure 2.2. Representative sediment grabs of Lucinda area. The map shows grab positions and bottom topography.

2.2.8. Assumptions of the model

A model is a simplified representation of the real world that attempts to capture as much of the world's heterogeneity as possible, and as such, assumptions are inherent in it. The current model is no exception; the following assumptions were adopted in the settings of the present model:

- Waters are considered vertically homogeneous or optically shallow
- Transformation of reflectance just above the water to subsurface reflectance is independent of the viewing geometry of the sensor
- There is no inelastic scattering or other source of light (e.g. fluorescence) within the water body

- Seawater, phytoplankton, coloured dissolved organic matter, mineral (inorganic) particles and detritus are the major colouring constituents in surface waters
- Chlorophyll_*a* concentration is a proxy for total chlorophyll concentration.

The last point was addressed in section 2.2.3. Other assumptions are discussed in more detail below.

Water homogeneity

The optical properties derived from the model represent average values weighted over the optical depth. This approach is relevant for both homogeneous water columns and for very turbid waters, where reflectance is related to the optical properties of a thin upper surface layer and vertical inhomogeneities in the water properties can be ignored (Ouillon 2003). Errors between modelled and measured absorption and backscattering coefficients may arise in highly stratified surface waters, for instance under the conditions of submerged CHL maximum or photobleached CDOM in the thin surface layer. As a result, several studies have considered optical applications for stratified waters (Tassan 1997; Deng et al 2003; Ouillon 2003). In situ measurements in the present study area, however, suggest that this is not the case in Lucinda waters (see section 3.1).

Viewing geometry effects

Equation 2.6 relates remote sensing reflectance just above the water surface to its subsurface counterpart. The water-to-air divergence factor in this expression was derived for nadir viewing sensors (Lee et al 1998), although in reality the parameters involved in the relation (e.g. water-to-air internal reflection coefficient and ratio of upwelling subsurface irradiance to upwelling subsurface radiance) are functions of sensor viewing angles. The maximum error in remote sensing reflectance just above the water surface due to this assumption is 15 % for cases of turbid waters and large viewing angles (i.e. edges of the sensor scan) (Lee et al 1999). By choosing images with smaller viewing angles (direct overpass), these errors can be reduced.

Inelastic processes

Transspectral (inelastic) optical processes such as Raman scattering as well as fluorescence from chlorophyll and coloured dissolved organic matter are neglected in the model. For case I waters Raman scattering by water molecules was estimated to contribute up to 8 % to water-

leaving radiance (Gordon 1999). However, for case II waters it was found that Raman scattering had a small impact on the radiometric colour characteristics, such as water-leaving radiance (Pozdnyakov et al 2003). In case I non-turbid waters the contribution of chlorophyll fluorescence to the total upwelled radiance at the surface in the 670-690 nm region can vary between 10 % and 40 % under various environmental conditions (Culver et al 1997). The fluorescence contribution of CDOM to reflectance is most significant in the blue-green region of the visible spectrum and depends strongly on the presence of other water-colouring constituents. It ranges from 14 % in sediment- and chlorophyll-poor and CDOM-intermediate (CDOM absorption at 440 nm is 0.5 m^{-1}) waters to 4 % in fully oligotrophic (low levels of all water-colouring constituents) and mesotrophic waters (medium levels of all water-colouring constituents) (Vodacek et al 1994). At the same time, suspended sediments are efficient in "damping" the fluorescence effects of both CHL and CDOM, with their effects rapidly reduced by the introduction of scattering particles (Pozdnyakov et al 2003). In Lucinda waters, suspended sediments are expected to have a significant contribution to the underwater light field; therefore, fluorescence of CDOM and chlorophyll as well as Raman scattering can be ignored.

Water-colouring components not included in the model

In the present bio-optical model, seawater, phytoplankton, coloured dissolved organic matter, minerals particles and detritus are the major colouring constituents in the surface waters. Other potentially optically significant components include air bubbles, zooplankton, bacteria and viruses.

Air bubbles arising from air–sea interactions in moderate to high wind conditions are usually described as non-absorbing spheres in bio-optical models and hence should be included in the backscattering term (Zhang et al 2002). However, the optical effect of air bubbles at the concentrations usually encountered in the sea has been estimated as negligible at wind speeds up to 11 m/s (Stramski et al 2001). Since wind velocities at the end of the Lucinda jetty exceed 10 m/s less than 2 % of the time on average (Australian Bureau of Meteorology, e-mail communication), for the purposes of the present study the contribution of air bubbles to water-leaving radiance is ignored.

Since zooplankton are grazers of phytoplankton, chlorophyll is invariably present within their digestive tracts, suggesting that the absorption and backscattering of zooplankton might display optical features similar to those of phytoplankton. However, zooplankton

concentrations in the ocean are generally very low in comparison to phytoplankton and as such, this component is considered optically ineffective (Pozdnyakov et al 2003).

Concentrations of bacterioplankton can reach 10^9 cells per cm^3 in eutrophic waters (Bukata et al 1995), potentially contributing to the underwater light field. Heterotrophic (meaning depending on external sources of organic compounds) bacteria have a representative size of 0.55 μm, while viral particles or viruses are usually smaller than 0.1 μm (Stramski et al 2001). Therefore, with the current in vitro filtering standards, both components are routinely attributed to a dissolved pool, which leads to overestimation of the absorption of dissolved matter. However, the CDOM absorption measurement procedure accounts for possible contamination of a sample by spectrally neutral scattering substances (see section 3.1.2, methodology). On the other hand, underestimation of TSS concentration and hence its backscattering properties is another consequence of neglecting particles smaller than the filter pore size. However, most of the particle backscatter that would be encountered by light in natural waters is due to particles of diameter greater than 2 μm, since smaller particles have a lower scattering efficiency (Kirk 1994). Moreover, a recent modelling study suggests that the contribution of microorganisms has little importance for backscattering in natural waters (Stramski et al 2001). Due to the above considerations, these organisms are not explicitly included in the current model.

2.2.9. Inversion of the bio-optical model

Given satellite-derived water-leaving radiances, it is desirable to determine concentrations of chlorophyll, suspended sediments, and dissolved organics that will generate water-leaving radiances most closely resembling the remotely sensed spectrum. In the present inverse approach, the least distance technique is employed whereas the aquatic concentrations in question are varied in an iterative manner until a "best fit" radiance spectrum is produced that optimally replicates the corresponding satellite-derived values.

The actual procedure for estimating "best fit" concentrations of water-colouring substances is as follows. Using the bio-optical model described above (Table 2.1), a database of water constituents and corresponding water-leaving radiances is created over the ranges of CHL (0.1-3 mg/m^3 at a 0.1 mg/m^3 resolution, 3-5 mg/m^3 at a 0.2 mg/m^3 resolution, 5-10 mg/m^3 at a 0.5 mg/m^3 resolution and 10-30 mg/m^3 at a 1 mg/m^3 resolution), TSS concentration (the same as for CHL except that the units are g/m^3), $a_{CDOM}(440)$ (0.01-0.1 m^{-1} at a 0.01 m^{-1} resolution, 0.1-1 m^{-1} at a 0.05 m^{-1} resolution, 1-5 m^{-1} at a 0.5 m^{-1} resolution) and optical parameters as defined in Table 2.1. Some spectra were eliminated from the database to avoid physically

unrealistic scenarios in Lucinda waters. The condition for such elimination was that the CHL equivalent of TSS, SS_{CHL} (equation 2.14), is less than the TSS concentration (otherwise negative CHL-corrected TSS concentration would be obtained in equation 2.16):

$$[SS_{CHL}] < [TSS]. \qquad (2.18)$$

Parameter	**symbol**	**min**	**max**	**average**	**step**	**unit**
Chlorophyll specific absorption	$a^*_{ph}(440)$	0.02	0.14	0.08	0.02	m^2/mg
Non-CHL particulates absorption	a^*_{np}	0.01	0.1	0.04	0.02	m^2/g
Exponential slope of non-CHL particulates	S_{np}	0.005	0.013	0.009	0.004	nm^{-1}
TSS specific backscatter	bb^*_{TSS}	0.005	0.036	0.02	0.007	m^2/g
Exponential slope of CDOM	S_{CDOM}	0.011	0.023	0.015	0.004	nm^{-1}
Spectral slope of backscatter of TSS *	γ	0.8	1.25	1	0.05	DL
Chlorophyll	CHL	0.1	30	NA	See text	mg/m^3
Total suspended sediments	TSS	0.1	30	NA	See text	g/m^3
CDOM absorption at 440 nm	$a_{CDOM}(440)$	0.01	5	NA	See text	m^{-1}

Table 2.1. Parameters and their ranges used in the model. DL stands for dimensionless.
* Spectral slope of backscatter of TSS is set constant at its average value, as the bio-optical model is insensitive to its variations (for explanation see section 2.3.3).

The input SeaWiFS water-leaving spectrum is then compared with all radiance spectra in the database (total 264,114,000). The program looks first for the maximum distance between the SeaWiFS $nLw_{SeaWiFS}(\lambda)$ and the modelled $nLw_{model}(\lambda)$ water-leaving radiances within each pair of spectra. It then finds the least such distance among all available combinations of SeaWiFS and modelled spectra. The modelled spectra corresponding to this least distance is a solution with associated values of CHL, TSS, $a_{CDOM}(440)$ and 5 optical parameters (total of 8 unknowns since the slope of particulate backscatter is set constant):

$$\underset{MV}{Min}\,\underset{\lambda}{Max}[Dist(MV,\lambda)], \qquad (2.19)$$

where MV represents model variables (CHL, TSS, $a_{CDOM}(440)$ and optical parameters); discrete wavelengths λ correspond to the SeaWiFS bands 1 through 8 (412 nm, 443 nm, 490 nm, 510 nm, 555 nm, 670 nm, 765 nm, 865 nm); and

$$Dist = abs\ \{\ nLw_{SeaWiFS}(\lambda) - nLw_{model}(\lambda)\ \}. \qquad (2.20)$$

Advantages of the inversion method applied in this study include transparency and straightforwardness of application in other environments. The latter might require other

parameter and properties ranges. By iterating through the whole set of over 250 million spectra, the procedure ensures that the absolute minimum of the difference between the calculated and the measured radiances is achieved. The main disadvantage of this approach is the substantial computational time required. If operational processing were desired, a more efficient inversion scheme should be used. Possible solutions are discussed in Chapter 5.